

## Analyzing Surface Code as Error Correction Method for Quantum Gate Translation of a Classical Arithmetic Logic Unit (ALU) in the Presence of Depolarizing Noise

Shani Marish V. Pineda<sup>1</sup>, Kenneth D. Cabobos<sup>2</sup>, Brent Neilson P. Rebulanan<sup>3</sup>,  
Joshua Benjamin B. Rodriguez<sup>4</sup> and Orland D. Tubola<sup>5</sup>

### ABSTRACT

Quantum computing holds promise, but maintaining quantum information integrity is challenging. This study evaluates surface codes for error correction in a quantum ALU using IBM Qiskit. Simulations under depolarizing noise show surface codes reduce errors and enhance accuracy. For the NAND Gate, state  $|1\rangle$  error dropped from 18.57% to 10.78% and state  $|0\rangle$  from 56.3% to 32.68%. For the NOR Gate, state  $|0\rangle$  error fell from 23.38% to 6.62% and state  $|1\rangle$  from 70.87% to 20.08%. For the XNOR Gate, errors for states  $|0\rangle$  and  $|1\rangle$  decreased from 5.08% to 2.54%. For the Full Adder, state  $|00\rangle$  error decreased from 99.19% to 83.74% and state  $|10\rangle$  from 31.3% to 22.02%, but increased for states  $|01\rangle$  from 17.63% to 22.11% and  $|11\rangle$  from 43.75% to 44.44% due to the added complexity of the circuit. This advancement in fault-tolerant quantum computing paves the way for solving problems beyond the capabilities of classical computing.

**DOI:** 10.37936/ecti-cit.2025191.257554

### Article information:

**Keywords:** Quantum Computing, Quantum Error Correction, Surface Code, Fault Tolerance, IBM Qiskit

### Article history:

Received: July 15, 2024  
Revised: September 5, 2024  
Accepted: December 12, 2024  
Published: January 4, 2024  
(Online)

### 1. INTRODUCTION

Quantum computing is an emerging technology with the potential to achieve results beyond classical computing methods. It offers a new approach to tackle challenges addressing the growing demands for solutions to increasingly complex problems [1]. Due to its capability of processing data at an exponential rate, researchers are getting more attracted to exploring the possible extensive range of applications [2].

One area where quantum computing opens up new possibilities is in revolutionizing complementary metal-oxide-semiconductor (CMOS) technology [3]. This has led to promising quantum computing technology alternatives, like reversible logic and quantum-dot cellular automata (QCA) technology, offering higher speed, lower power consumption, and reduced complexity [4,5]. These advancements translate basic classical circuit functions into quantum circuits, outperforming their classical counterparts and handling quantum-specific operations [6].

Several studies have demonstrated the creation of

quantum circuits like arithmetic logic units (ALUs) to enhance the computational capabilities of central processing units (CPUs) [7-10]. Despite ongoing research and development aimed at creating high-performance quantum ALUs, the realization of these quantum circuits are being hindered by noise, decoherence, and implementation imperfections [11]. Quantum error correction (QEC) methods are essential to enable fault-tolerant quantum computing, as these errors can hinder the progress and effectiveness of quantum computing [2].

Surface code is one of the most promising QEC methods. It works by increasing the number of physical qubits to encode a logical qubit, distributing quantum information across larger qubits [12]. This redundancy allows error detection and correction, paving the way for fault-tolerant quantum computation [13].

In implementing QEC methods, researchers often utilize Qiskit, an open-source software developed by International Business Machines (IBM) Corporation.

<sup>1,2,3</sup>The authors are with the Polytechnic University of the Philippines, Philippines, Email: shanimarish@gmail.com, caboboskennethzxc@gmail.com and rebulanan.brent@gmail.com

<sup>4</sup>The author is with the Department of Computer Engineering, Polytechnic University of the Philippines, Philippines, Email: jbbrodriguez@pup.edu.ph

<sup>5</sup>The author is with the Research Institute for Strategic Foresight and Innovation, Polytechnic University of the Philippines, Philippines, Email: odtubola@pup.edu.ph

<sup>1</sup>Corresponding author: shanimarish@gmail.com

Qiskit, an open-source software developed by International Business Machines (IBM) Corporation. Qiskit enables users to write code using Python and run experiments on quantum computers [14]. It offers tools to create, manipulate, and simulate quantum registers, circuits, and algorithms, making it easier to design and implement quantum applications [15,16]. Using Qiskit, researchers can test the fault tolerance of surface codes in real-world scenarios and assess their effectiveness on actual quantum hardware [17].

The main objective of this study is to analyze the fault tolerance of surface code in a quantum arithmetic logic unit (ALU) under the presence of depolarizing noise. The ALU consists of NAND, NOR, and XNOR gates for the logic unit and a full adder for the arithmetic unit, all within a 4:1 multiplexer. The researchers aim to evaluate the robustness of surface codes against noise and determine the level of fault tolerance achievable. They will use the IBM Qiskit platform to simulate the circuits that will be used to build the quantum ALU, assessing the performance of surface codes in these circuits.

## 2. RELATED WORKS

### 2.1 Quantum Arithmetic Logic Unit (ALU)

With ongoing technological innovations and the growing need to solve complex problems, there has been an increase in interest and investment in quantum computing. Major technology companies such as Google, IBM, Rigetti, Intel, IonQ, and Xanadu are investing in this field, recognizing its potential to revolutionize various industries [18].

Researchers are currently exploring quantum computing as an alternative to complementary metal-oxide-semiconductor (CMOS) technology. While CMOS has been the primary technology for digital circuit design, it faces challenges related to heat dissipation and scaling limitations [19]. Quantum-dot cellular automata (QCA) technology is a promising substitute for CMOS, especially for building important circuits such as full adders and Arithmetic Logic Units (ALUs).

QCA technology uses the position of electrons to represent binary information, enabling extremely compact and low-power circuit designs. This capability is particularly beneficial for circuits like full adders, which are crucial components in Arithmetic Logic Units (ALUs) responsible for performing mathematical operations within digital circuits [20]. Optimized designs of full adders have been created using QCA technology, showcasing reduced complexity, area, latency, and power consumption compared to traditional designs [21, 22].

The development of efficient full adders paves the way for constructing more complex circuits, such as ALUs. ALUs, which rely on full adders for performing arithmetic operations, benefit from advancements in QCA technology. Studies [7, 9, 10] highlight the

advantages of QCA technology over CMOS in developing ALUs. Study [7] developed a logically and physically reversible ALU based on QCA, notably reducing energy dissipation and increasing energy efficiency. Similarly, a study [9] presented a QCA multilayer ALU that outperformed CMOS designs in cell number, area, latency, and power consumption. A study [10] also demonstrated that QCA technology improved quantum cost, reduced the number of cells, and minimized the occupied area for quantum ALUs. These studies demonstrate that QCA offers a promising alternative to CMOS technology.

The prospect of constructing a fully functional quantum ALU, founded on classical operations transposed into quantum circuits, presents a promising frontier in computational technology [8].

### 2.2 Fault-tolerant Quantum Computing

Quantum systems are sensitive to various errors, noise, and imprecisions, which can disrupt the quality of computations [23]. To address these challenges, fault-tolerant quantum computing is crucial for reliable quantum information processing. It involves adding extra qubits and logical gates to make circuits robust against errors like bit-flips, phase-flips, and depolarizing noise [24, 25]. This approach ensures that quantum computations can proceed accurately even in the presence of errors.

Using quantum error correction (QEC) codes helps overcome the inherent fragility of quantum systems [25]. Prominent QEC codes include surface, Shor, Steane, and stabilizer codes [26].

Shor's code is a quantum error correction method that encodes a single logical qubit into nine physical qubits, allowing it to correct arbitrary single-qubit errors. A study revealed that Shor codes are degenerate, with three pairs of similar syndromes involving Z errors, yet they can still correct all single-qubit errors [27].

Steane's code constructs quantum codes from classical block codes, improving quantum code parameters by increasing dimension while maintaining error protection [28]. Its application to Bose–Chaudhuri–Hocquenghem (BCH) and algebraic geometry codes further enhances quantum communication and computation systems, making it a significant advancement in QEC.

Stabilizer codes protect quantum information by encoding qubits into a larger system which are defined by an abelian subgroup of the Pauli group [29]. These preserve the encoded state, allowing for detecting and correcting errors without measuring the quantum information directly, which is essential for practical quantum computing and communication systems.

By leveraging these QEC codes, quantum systems can achieve greater robustness and reliability, paving the way for more practical and scalable quantum computing applications.

### 2.3 Surface Code as Quantum Error Correction (QEC)

Surface codes are a robust method for quantum error correction, essential for practical quantum computers [12,13]. It utilizes a two-dimensional lattice of qubits to identify and correct errors during quantum operations. These codes are particularly effective for systems with qubits arranged in a 2D grid, utilizing local interactions for efficient error management.

The resilience of surface codes to coherent noise highlights their potential for real-world quantum computing applications [30]. Recent research has further explored this potential by demonstrating the effectiveness of partitioning surface codes and transmitting them via multiple paths in fault-tolerant quantum communications. This innovative approach enhances communication fidelity and optimizes resource utilization while maintaining a fidelity threshold. Evaluations through simulations illustrate significant improvement in communication fidelity compared to other models, underscoring the promise of surface codes in practical quantum communication systems [31].

## 3. METHODS

The quantum gate translation of a classical CMOS 1-bit ALU is simulated using IBM Qiskit, a software designed for powerful executions on IBM quantum computers. The quantum gate translation involved using NAND, NOR, and XNOR gates for the logic unit and a full adder for the arithmetic unit, with the logical operations controlled by a 4:1 multiplexer. Qiskit Aer, a library within the Qiskit framework, was primarily used to simulate the behavior of quantum circuits both under normal conditions and with the addition of depolarizing noise.

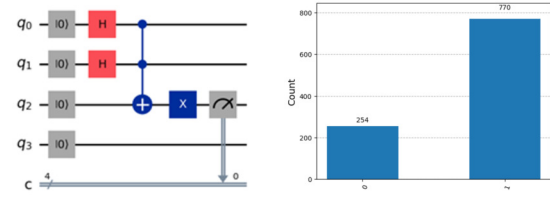
The research study involves five Jupyter notebooks: (1) the NAND quantum circuit, NAND quantum circuit with depolarizing noise, and NAND quantum circuit with surface code then noise; (2) the NOR quantum circuit, NOR quantum circuit with depolarizing noise, and NOR quantum circuit with surface code then noise (3) the XNOR quantum circuit, XNOR quantum circuit with depolarizing noise, and XNOR quantum circuit with surface code then noise; (4) the Full-Adder quantum circuit, Full-Adder quantum circuit with depolarizing noise, and Full-Adder quantum circuit with surface code then noise; (5) the realization of a 4:1 multiplexer and a quantum ALU.

### 3.1 Development of 1-bit ALU Quantum Gate Circuits

In creating the quantum equivalents of the three logical gates and a full adder, a reset function was implemented before the quantum gates to ensure the qubits started in the state of 0 before the quantum computation began. Hadamard gates were utilized

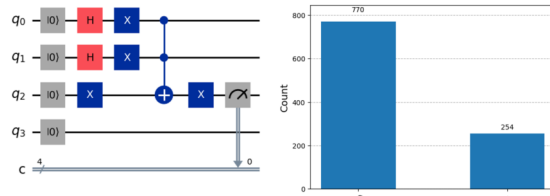
to translate classical gates into quantum gates, placing the qubits in a superposition state and allowing the measurement of the split probabilities of the circuit outcomes. All the quantum circuits for the logical operations, NAND, NOR, and XNOR, were described by four qubits and one classical register. The full adder quantum circuit used the same number of qubits but included two classical registers, one for the sum and the other for the carry.

Figure 1 shows the quantum gate translation of the NAND operation. The circuit used a Toffoli gate with the first two qubits ( $q_0$  and  $q_1$ ) as control qubits and the third qubit ( $q_2$ ) as the target qubit. A Pauli-X gate was added after the target qubit. The state of the third qubit ( $q_2$ ) was measured and recorded in the classical register ( $c$ ) as the output of the NAND operation.



**Fig.1:** Quantum Gate Translation of NAND Operation and its Split Probability.

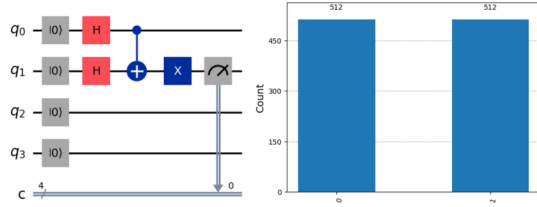
Figure 2 displays the quantum gate translation of the NOR operation. The circuit also used a Toffoli gate with the first two qubits ( $q_0$  and  $q_1$ ) as control qubits and the third qubit ( $q_2$ ) as the target qubit. Each of the first three qubits ( $q_0$ ,  $q_1$ , and  $q_2$ ) had a Pauli-X gate applied to them before the Toffoli gate operation. This was followed by another Pauli-X gate applied to the target qubit ( $q_2$ ) after the Toffoli gate operation. The third qubit ( $q_2$ ) was measured, and the output of the NOR operation was recorded in the classical register ( $c$ ).



**Fig.2:** Quantum Gate Translation of NOR Operation and its Split Probability.

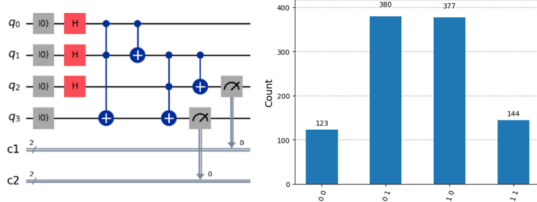
Figure 3 illustrates the quantum gate translation of the XNOR operation. A CNOT gate was used with the first qubit ( $q_0$ ) as the control qubit and the second qubit ( $q_1$ ) as the target qubit, cascaded with a Pauli-X gate. The result of the XNOR operation was measured by getting the state of the second qubit ( $q_1$ ) which was recorded in the classical register ( $c$ ).

Figure 4 depicts the quantum gate translation of the full-adder operation. The full-adder circuit in-



**Fig.3:** Quantum Gate Translation of XNOR Operation and its Split Probability.

volved multiple Toffoli and CNOT gates with different combinations of control and target qubits to perform the necessary bitwise addition operations. The state of the fourth qubit ( $q_3$ ) was measured and recorded in the first classical register ( $c_1$ ) as the sum, while the state of the third qubit ( $q_2$ ) was measured and recorded in the second classical register ( $c_2$ ) as the carry.



**Fig.4:** Quantum Gate Translation of Full Adder Operation and its Split Probability.

Figures 1, 2, 3, and 4 also present the split probabilities of each quantum gate translation. Each circuit was simulated for 1024 counts, and the split probabilities matched the expected outcomes from the truth table of its classical counterpart.

### 3.2 Development of 1-bit ALU Quantum Gate Circuits with Surface Code

The quantum gate translations with surface code for the NAND, NOR, and XNOR circuits are shown in Figures 5, 6, and 7, respectively. These were created by applying three additional ancilla qubits to the four data qubits. Incorporating the surface code involved using X-type and Z-type stabilizers to detect errors. For X-type stabilizers, Hadamard gates were applied to the ancilla qubits, followed by CNOT gates between the ancilla and data qubits, and then measuring the ancilla qubits to detect bit-flip errors. For Z-type stabilizers, CNOT gates were directly applied between the data qubits and ancilla qubits, and then the ancilla qubits were measured to detect phase-flip errors. Stabilizer measurements provided information about the presence of bit-flip or phase-flip errors by reflecting changes in the ancilla qubits, allowing for error detection without disturbing the quantum state of the data qubits. The data qubits were then measured to obtain the logical gate output while ensuring error robustness through the surface code.

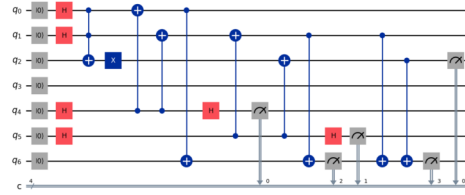


**Fig.5:** NAND Quantum Circuit with Surface Code.

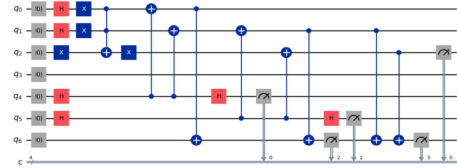


**Fig.6:** NOR Quantum Circuit with Surface Code.

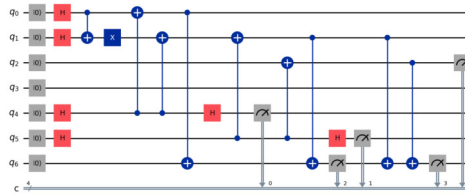


**Fig.7:** XNOR Quantum Circuit with Surface Code.

Implementing surface code in the quantum circuit of a full adder was slightly different. In the circuit shown in Figure 8, five additional ancilla qubits and an additional classical register were added to the four data qubits and two classical registers for sum and carry. Like in the three logical gates, X-type and Z-type stabilizers were also applied to detect bit-flip and phase-flip errors. The circuit concluded by measuring the data qubits to obtain the final computational results.

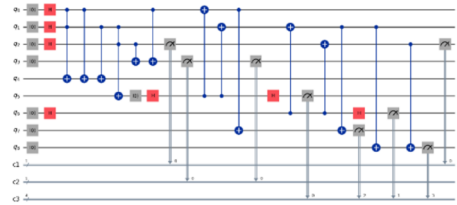


**Fig.8:** Full Adder Quantum Operation with Surface Code.

### 3.3 Testing

Figure 9 outlines the research process. The NAND, NOR, XNOR, and full adder quantum circuits were simulated with and without surface codes to assess error correction capabilities. The depolarizing noise model, implemented through the depolarizing\_error function in Qiskit, was used to simulate real quantum noise in the circuit, impacting measurement accuracy. This noise mirrors real-world disturbances

in quantum systems and is essential for assessing error correction methods and strategies.

Each circuit is simulated using IBM Qiskit, with each simulation repeated for a total of 1024 times. The circuits were first tested without error correction to observe the effects of noise and generate histograms of the results. Surface codes were then applied to the circuits before simulating noise again, creating a second set of histograms for comparison. The researchers then analyzed how well the surface codes reduced the impact of noise. They compared histograms from circuits with and without surface codes to determine the effectiveness of surface codes in maintaining the integrity of quantum computations against noise.

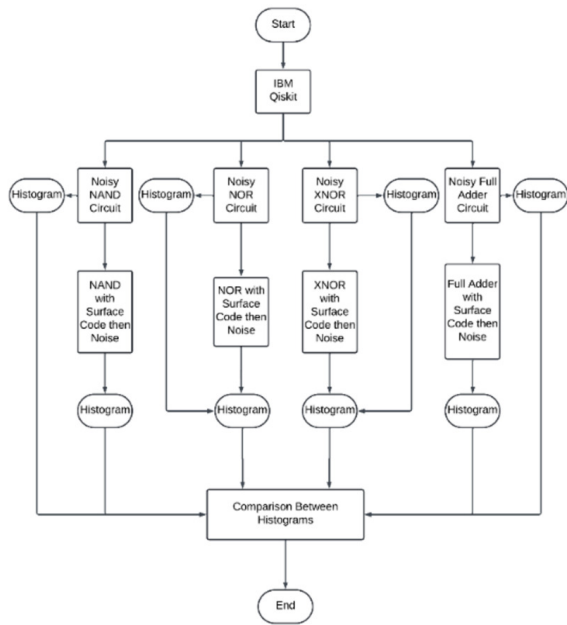


**Fig.9:** Flowchart Diagram.

## 4. RESULTS AND DISCUSSION

The researchers used histograms to illustrate the simulated circuits and interpret the results easily. The histograms display how often a specific state is an output in 1024-count circuit simulations. When simulating a quantum circuit, results may vary slightly each time due to the probabilistic nature of Hadamard gates, which create superposition states. This inherent randomness ensures consistently similar results despite minor variations.

Histograms of original quantum circuits without surface code show a distinct output state from the simulation of the three logical gates quantum circuit, which has only 2 output states, and the full adder operation, which has only 4 output states. When surface code is applied to the original quantum circuits, the researchers noticed increased states from the histograms. The quantum circuits applied with surface code tend to collapse into 16 possible states, as indicated by the figures of the logical NAND, NOR, and XNOR gates depicted in Figures 11, 13, and 15. In comparison, the full adder operation, shown in Figure 17, collapses into 64 possible states. This increase is due to the surface code spreading quantum information across many qubits and using multiple layers of redundancy to detect and correct errors. This process introduces additional possible outcomes because of the greater number of qubits and interactions involved. Additionally, adding more qubits to a quantum system introduces additional sources of errors, which can accumulate and affect overall performance [12].

The histograms for logical NAND, NOR, and XNOR gates, as presented in Figures 10, 11, 12, 13, 14, and 15, were interpreted by calculating each quantum circuit's split probabilities for Output 0 ( $|0000\rangle$ ) and Output 1 ( $|0001\rangle$ ). The final count for Output 0 and Output 1 was obtained by adding together all the state probabilities measured by the last measurement gate that resulted in Output 0, and the same was done for Output 1. In contrast, the histograms for a full adder, shown in Figures 16 and 17, were interpreted by focusing on the last two qubits of the quantum state, which represent the sum and carry-out qubits. The counts for these two qubits were categorized into four possible output states:  $|00\rangle$ ,  $|01\rangle$ ,  $|10\rangle$ , and  $|11\rangle$ .

The percentage error was then calculated, which measures the discrepancy between observed and expected values. This involved comparing the observed results of quantum circuits with noise (shown in Figures 10, 12, 14, and 16) and quantum circuits with surface code then noise (shown in Figures 11, 13, 15, and 17) to the expected results of the original quantum circuits (shown in Figures 1, 2, 3, and 4).

The comparison of the percent error between the quantum circuits with noise and the quantum circuits with surface code then noise served as the basis to evaluate the effectiveness of the surface code as a quantum error correction method. This analysis aimed to determine if the surface code successfully reduced noise and contributed to creating fault-tolerant circuits that maintained quantum information integrity.

### 4.1 Circuit Simulation of NAND

In the simulation of the four-qubit NAND Quantum Circuit with Noise, the  $|0000\rangle$  state (representing  $|0\rangle$ ) had a count value of 397, while the  $|0001\rangle$  state (representing  $|1\rangle$ ) had a count value of 627. The circuit created the states  $|0000\rangle$  and  $|0001\rangle$  with probabilities of 38.8% and 61.2%, respectively. These split probabilities are not close to the ideal case due to the noise, wherein the state  $|0000\rangle$  has a percent error of 56.3%, while the state  $|0001\rangle$  has an error of 18.57%.

The seven-qubit NAND Quantum Circuit with Surface Code then Noise, shows more split probabilities due to the additional ancilla qubits. The sum for

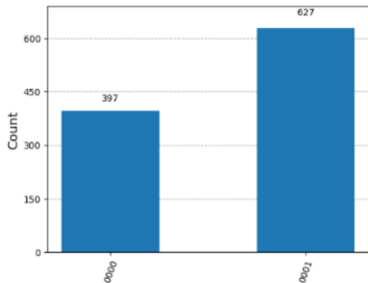


**Fig.10:** Result of NAND Quantum Circuit with Noise.

Output 1 (representing the  $|0001\rangle$  state) results in 687 counts, and the sum for Output 0 (representing the  $|0000\rangle$  state) results in 337 counts. The percent error for the sum of Output 1 is 10.78%, and for the sum of Output 0 is 32.68%.

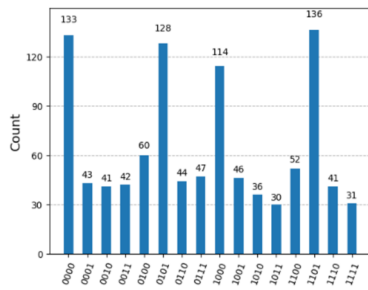


**Fig.11:** Result of NAND Quantum Circuit with Surface Code then Noise.

Table 1 summarizes the output states for NAND Gate. For the 1024 shot counts, the expected output should be 770 for the sum of Output 1 and 254 for the sum of Output 0.

**Table 1:** Measurement of Output States for NAND Gate.

Quantum Circuit (QC) of NAND	QC with Depolarizing Noise		QC with Surface Code then Depolarizing Noise		
$ 0000\rangle$	254	$ 0000\rangle$	397	$ 0000\rangle$	337
$ 0001\rangle$	770	$ 0001\rangle$	627	$ 0001\rangle$	687
<b>Total</b>	1024	<b>Total</b>	1024	<b>Total</b>	1024

Comparing the two simulations, the surface code implementation reduces the percent error for Output 1 from 18.57% to 10.78% and Output 0 from 56.3% to 32.68% as shown in Table 2 below.

**Table 2:** Measurement of Percent Error when Compared to Split Probabilities of NAND Quantum Circuit.

	QC with Depolarizing Noise	QC with Surface Code then Depolarizing Noise
$ 0000\rangle$	56.3%	32.68%
$ 0001\rangle$	18.57%	10.78%

## 4.2 Circuit Simulation of NOR

In the case of the four-qubit NOR Quantum Circuit with Noise, the  $|0000\rangle$  state (representing  $|0\rangle$ ) had 590 counts, and the  $|0001\rangle$  state (representing  $|1\rangle$ ) had 434 counts. The circuit generated the  $|0000\rangle$  and  $|0001\rangle$  states with probabilities of 57.61% and 42.38%, respectively. These probabilities differ from the ideal case due to noise, resulting in a percent error of 23.38% for the  $|0000\rangle$  state and 70.87% for the  $|0001\rangle$  state.

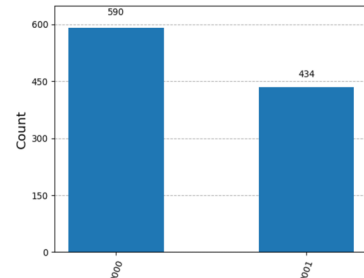


**Fig.12:** Result of NOR Quantum Circuit with Noise.

For the seven-qubit NOR Quantum Circuit with Surface Code then Noise, additional split probabilities arise due to the inclusion of ancilla qubits, similar to the NAND Quantum Circuit with Surface Code. The expected output should be 590 for the sum of Output 0 (representing the  $|0000\rangle$  state) and 434 for the sum of Output 1 (representing the  $|0001\rangle$  state), out of a total of 1024 counts. In the actual results, the sum for Output 0 is 719 counts, and the sum for Output 1 is 305 counts. Comparing the expected and actual distributions, Output 0 has 590 expected counts and 719 actual counts, resulting in a percent error of 6.62%. Output 1 has 434 expected counts and 305 actual counts, resulting in a percent error of 20.08%.

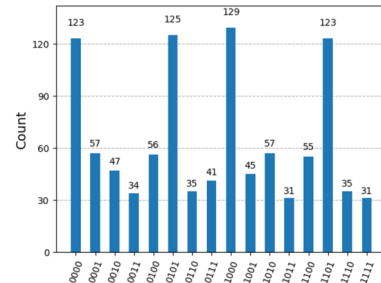


**Fig.13:** Result of NOR Quantum Circuit with Noise.

Table 3 summarizes the output states for NOR Gate. For the 1024 shot counts, the expected output should be 254 for the sum of Output 1 and 770 for the sum of Output 0.

The surface code implementation reduces the percent error for Output 0 from 23.38% to 6.62% and for

**Table 3:** Measurement of Output States for NOR Gate.

<i>Quantum Circuit (QC) of NOR</i>		<i>QC with Depolarizing Noise</i>		<i>QC with Surface Code then Depolarizing Noise</i>	
$ 0000\rangle$	770	$ 0000\rangle$	590	$ 0000\rangle$	719
$ 0001\rangle$	254	$ 0001\rangle$	434	$ 0001\rangle$	305
<b>Total</b>	1024	<b>Total</b>	1024	<b>Total</b>	1024

Output 1 from 70.87% to 20.08% as shown in Table 4 below.

**Table 4:** Measurement of Percent Error when Compared to Split Probabilities of NOR Quantum Circuit.

	<i>QC with Depolarizing Noise</i>	<i>QC with Surface Code then Depolarizing Noise</i>
$ 0000\rangle$	23.38%	6.62%
$ 0001\rangle$	70.87%	20.08%

#### 4.3 Circuit Simulation of XNOR

In the four-qubit XNOR Quantum Circuit simulation with Noise, the  $|0000\rangle$  (representing  $|0\rangle$ ) state had 538 counts, while the  $|0001\rangle$  (representing  $|1\rangle$ ) state had 486 counts. These counts correspond to probabilities of 52.5% and 47.5%, respectively. These probabilities are close to the expected output of the XNOR operation, which ideally produces 512 counts for both  $|0000\rangle$  and  $|0001\rangle$  states. The percent error is not high, wherein the state  $|0000\rangle$  has an error of 5.08% and  $|0001\rangle$  has an error of 5.54%.

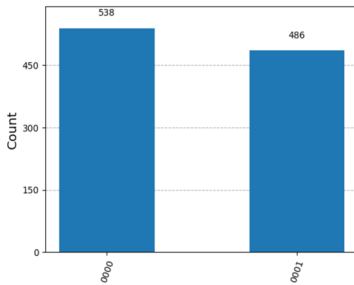


**Fig.14:** Result of XNOR Quantum Circuit with Noise.

The introduction of additional ancilla qubits in the seven-qubit XNOR Quantum Circuit with Surface Code then Noise also leads to an increase in split probabilities. The total output counts correspond to the number of shots, totalling 1024. The expected output should be 512 for the sum of Output 0 (representing the  $|0000\rangle$  state) and 512 for the sum of Output 1 (representing the  $|0001\rangle$  state). Actual Output 0 recorded 525 counts, while Output 1 recorded 499 counts. Upon comparing the expected and actual distributions, Output 0 has a percent error of 2.54%, mirroring the same percent error for Output 1.

Table 5 summarizes the output states for XNOR Gate. For the 1024 shot counts, the expected out-

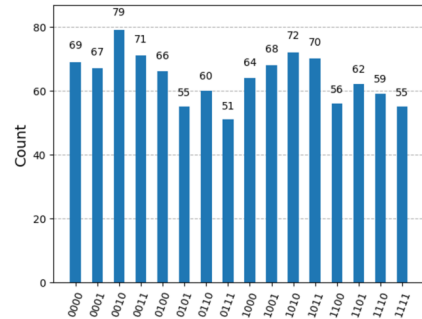


**Fig.15:** Result of XNOR Quantum Circuit with Surface Code then Noise.

put should be 512 for the sum of both Output 1 and Output 2.

**Table 5:** Measurement of Output States for XNOR.

<i>Quantum Circuit (QC) of XNOR</i>	<i>QC with Depolarizing Noise</i>	<i>QC with Surface Code then Depolarizing Noise</i>	
$ 0000\rangle$	512	$ 0000\rangle$	538
$ 0001\rangle$	512	$ 0001\rangle$	486
<b>Total</b>	1024	<b>Total</b>	1024

This surface implementation in XNOR Quantum Circuit reduces the percent error for both Output 0 and Output 1 from 5.08% to 2.54% as shown in Table 6 below.

**Table 6:** Measurement of Percent Error when Compared to Split Probabilities of XNOR Quantum Circuit.

	<i>QC with Depolarizing Noise</i>	<i>QC with Surface Code then Depolarizing Noise</i>
$ 0000\rangle$	5.08%	2.54%

#### 4.4 Circuit Simulation of Full Adder

The Full Adder Quantum Circuit with noise has four state probabilities compared to the three logic quantum gates: NAND, NOR, and XNOR. The simulation of the four-qubit full adder resulted in the state  $|00\rangle$  having 245 counts, the state  $|01\rangle$  having 313 counts, the state  $|10\rangle$  having 259 counts, and the state  $|11\rangle$  having 207 counts, resulting in a total of 1024 counts. These counts correspond to probabilities of 23.93%, 30.52%, 25.25%, and 20.24%, respectively. These probabilities are noticeably different compared to the expected output of the Full Adder operation, which ideally produces 123 counts for state  $|00\rangle$ , 380 counts for state  $|01\rangle$ , 377 counts for state  $|10\rangle$ , and 144 counts for state  $|11\rangle$ . The comparison between the expected outputs and actual outputs resulted in a percent error of 99.19% in state  $|00\rangle$ , 17.63% in state  $|01\rangle$ , 31.3% in state  $|10\rangle$ , and 43.75% in state  $|11\rangle$ .

Similar to the three previous logic gates, the inclusion of ancilla qubits in the nine-qubit Full Adder

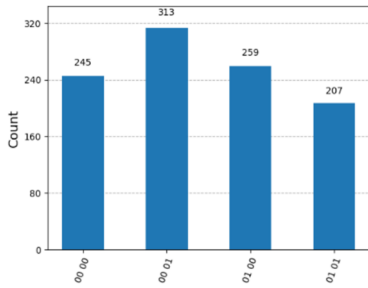


**Fig.16:** Result of Full Adder Quantum Circuit with Noise.

Quantum Circuit with Surface Code then Noise results in additional split probabilities. Comparing the expected and actual distributions,  $|00\rangle$  sum-carry out qubits has 123 expected counts and 226 actual counts, resulting in a percent error of 83.74%. The state  $|01\rangle$  has 380 expected counts and 296 actual counts, resulting in a percent error of 22.11%. The  $|10\rangle$  state has an expected count of 377 and 294 actual counts, resulting in a percent error of 22.02%. Lastly, the state  $|11\rangle$  has 144 expected and 208 actual counts, resulting in a 44.44% error.

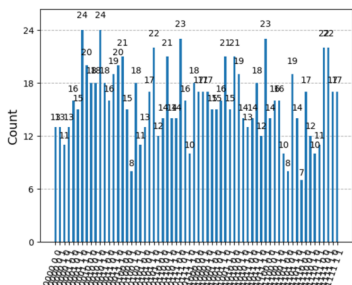


**Fig.17:** Result of Full Adder Quantum Circuit with Surface Code then Noise.

Table 7 summarizes the output states for the Full Adder. For the 1024 shot counts, the expected output should be 123 for  $|00\rangle$ , 380 for  $|01\rangle$ , 377 for  $|10\rangle$ , and 144 for  $|11\rangle$ .

**Table 7:** Measurement of Output States for Full Adder.

Quantum Circuit (QC) of Full Adder	QC with Depolarizing Noise		QC with Surface Code then Depolarizing Noise		
$ 00\rangle$	123	$ 00\rangle$	245	$ 00\rangle$	226
$ 01\rangle$	380	$ 01\rangle$	313	$ 01\rangle$	296
$ 10\rangle$	377	$ 10\rangle$	259	$ 10\rangle$	294
$ 11\rangle$	144	$ 11\rangle$	207	$ 11\rangle$	208
<b>Total</b>	1024	<b>Total</b>	1024	<b>Total</b>	1024

This surface implementation in Full Adder Quantum Circuit reduces the percent error for the state  $|00\rangle$  from 99.19% to 83.74% and for state  $|10\rangle$  from 31.3% to 22.02%. The sum and carry-out qubit result for  $|01\rangle$  didn't reduce the percent error after implementing surface code, which goes from 17.63% to

22.11%. Similarly to the state  $|11\rangle$ , the error went up from 43.75% to 44.44% as shown in Table 8 below. The increase in percent error for some states is likely due to the added complexity and ancilla qubits of surface codes, along with varying susceptibilities of different quantum states to noise.

**Table 8:** Measurement of Percent Error when Compared to Split Probabilities of Full Adder Quantum Circuit.

	QC with Depolarizing Noise	QC with Surface Code then Depolarizing Noise
$ 00\rangle$	99.19%	83.74%
$ 01\rangle$	17.63%	22.11%
$ 10\rangle$	31.3%	22.02%
$ 11\rangle$	43.75%	44.44%

## 5. CONCLUSION

This study explored the effectiveness of surface code as a quantum error correction method for creating a fault-tolerant quantum ALU, consisting of NAND, NOR, and XNOR gates for the logic unit and a full adder for the arithmetic unit.

The research team compared the percent error of the quantum circuits with and without surface code when noise was applied to the original quantum circuits without noise. The results showed that surface codes reduced noise in NAND, NOR, and XNOR circuits compared to their counterparts without surface codes. In contrast, the full adder quantum circuit with surface code reduced noise in some states but increased errors in others. This suggested that certain states were more susceptible to noise due to the added complexity and ancilla qubits.

Overall, the results demonstrated that the surface code implemented in the quantum circuits for creating a quantum ALU functioned effectively as an error correction method against depolarizing noise. The data revealed that the surface code reduced errors for most states in the quantum circuits, thereby enhancing the overall reliability of the quantum ALU.

## ACKNOWLEDGEMENT

First and foremost, the researchers would like to express their sincere gratitude to the Polytechnic University of the Philippines for fostering an environment that supports innovation and academic growth. The guidance and unwavering support from the university's faculty and staff played a crucial role in shaping the direction and success of this research.

Deepest appreciation is extended to the Department of Computer Engineering and the Research Institute for Strategic Foresight and Innovation (RISFI) at the university for their invaluable guidance, which greatly enhanced the quality of the research, particularly to the adviser and co-author for their consistent

mentorship and insightful contributions throughout the research process.

The researchers are equally grateful to their parents and friends, whose encouragement, patience, and understanding provided essential inspiration throughout this journey. Their support made the challenges more manageable and the milestones more meaningful.

Finally, special recognition goes to the Qiskit development team for their remarkable dedication to advancing technology. Their work provided the essential tools and resources that contributed significantly to the successful completion of this study.

## AUTHOR CONTRIBUTIONS

Conceptualization, S.P., K.C., and B.R.; methodology, S.P., K.C., and B.R.; software, S.P., K.C., and B.R.; validation, S.P., K.C., and B.R.; formal analysis, S.P., K.C., and B.R.; investigation, S.P., K.C., and B.R.; data curation, S.P., K.C., and B.R.; writing—original draft preparation, S.P., K.C., and B.R.; writing—review and editing, S.P., K.C., B.R., and O.T.; visualization, S.P., K.C., and B.R.; supervision, O.T. and J.R. All authors have read and agreed to the published version of the manuscript.

## References

- [1] H. Riel, “Quantum Computing Technology,” *2021 IEEE International Electron Devices Meeting (IEDM)*, San Francisco, CA, USA, pp. 1.3.1-1.3.7, 2021.
- [2] H. A. Bhat, F. A. Khanday, B. K. Kaushik, F. Bashir and K. A. Shah, “Quantum Computing: Fundamentals, Implementations and Applications,” in *IEEE Open Journal of Nanotechnology*, vol. 3, pp. 61-77, 2022.
- [3] R. Nikandish, E. Blokhina, D. Leipold and R. B. Staszewski, “Semiconductor Quantum Computing: Toward a CMOS quantum computer on chip,” in *IEEE Nanotechnology Magazine*, vol. 15, no. 6, pp. 8-20, Dec. 2021.
- [4] V. Bevara, S. Bevara, J. C. Prasad and M. K. Rvv, “Ultra low power reversible arithmetic processor based on quantum dot cellular automata,” *Authorea*, Apr. 2023
- [5] M. Alharbi, G. Edwards and R. Stocker, “Novel ultra-energy-efficient reversible designs of sequential logic quantum-dot cellular automata flip-flop circuits,” *The Journal of Supercomputing*, vol. 79, no. 10, pp. 11530–11557, Mar. 2023.
- [6] X. Zhu, J. Gu, H. Yin and Z. Wu, “Simulation of silicon quantum dots with diamond-channel by simplified ME model,” *Results in Physics*, vol. 38, p. 105575, Jul. 2022.
- [7] M. Alharbi, G. Edwards and R. Stocker, “Reversible quantum-dot cellular automata-based arithmetic logic unit,” *Nanomaterials*, vol. 13, no. 17, p. 2445, Aug. 2023.
- [8] B. Phillip, E. Butler, B. Ulrich and D. Carroll, “A quantum computing arithmetic-logic unit,” *Proceedings of the 2023 ACM Southeast Conference*, Apr. 2023.
- [9] S. Babaie, A. Sadoghifar and A. N. Bahar, “Design of an Efficient Multilayer Arithmetic Logic Unit in Quantum-Dot Cellular Automata (QCA),” in *IEEE Transactions on Circuits and Systems II: Express Briefs*, vol. 66, no. 6, pp. 963-967, June 2019.
- [10] B. Safaiezadeh, E. Mahdipour, M. Haghparast, S. Sayedsalehi and M. Hosseinzadeh, “Novel design and simulation of reversible ALU in quantum dot cellular automata,” *The Journal of Supercomputing*, vol. 78, no. 1, pp. 868–882, Jun. 2021.
- [11] S. Kurdziałek and R. Demkowicz-Dobrzański, “Measurement noise susceptibility in quantum estimation,” *Physical Review Letters*, vol. 130, no. 16, Apr. 2023.
- [12] R. Acharya *et al.*, “Suppressing quantum errors by scaling a surface code logical qubit,” *Nature*, vol. 614, no. 7949, pp. 676–681, Feb. 2023.
- [13] C. K. Andersen *et al.*, “Repeated quantum error detection in a surface code,” *Nature Physics*, vol. 16, no. 8, pp. 875–880.
- [14] R. Wille, R. Van Meter, and Y. Naveh, “IBM’s Qiskit tool chain: working with and developing for real quantum computers,” *Design, Automation & Test in Europe Conference & Exhibition (DATE)*, Mar. 2019.
- [15] D. Koch, L. Wessing and P. M. Alsing, “Introduction to coding quantum algorithms: a tutorial series using Qiskit,” 2019, *arXiv:1903.04359*.
- [16] E. h. Shaik and N. Rangaswamy, “Implementation of Quantum Gates based Logic Circuits using IBM Qiskit,” *2020 5th International Conference on Computing, Communication and Security (ICCCS)*, Patna, India, pp. 1-6, 2020.
- [17] A. Jayashankar, M. D. H. Long, H. K. Ng and P. Mandayam, “Achieving fault tolerance against amplitude-damping noise,” *Physical Review Research*, vol. 4, no. 2, Apr. 2022.
- [18] C. G. Almudever, L. Lao, R. Wille and G. G. Guerreschi, “Realizing quantum algorithms on real quantum computing devices,” *2020 Design, Automation & Test in Europe Conference & Exhibition (DATE)*, Mar. 2020.
- [19] C. Prasad, “A review of self-heating effects in advanced CMOS technologies,” *IEEE Transactions on Electron Devices*, vol. 66, no. 11, pp. 4546–4555, Nov. 2019.
- [20] B. C. Devnath and S. N. Biswas, “Low power Full Adder design using PTM Transistor model,” *Carpathian Journal of Electronic and Computer Engineering*, vol. 12, no. 2, pp. 15–20, Dec. 2019.
- [21] R. Laajimi, L. Touil and A. N. Bahar, “A novel efficient coplanar QCA full adder and full sub-

tractor design,” *International Journal of Electronics*, vol. 110, no. 8, pp. 1431–1446, Sep. 2022.

[22] M. A. Sohel, N. Zia, M. A. Ali and N. Zia, “Quantum computing based implementation of full adder,” *2020 IEEE International Conference for Innovation in Technology (INOCON)*, Nov. 2020.

[23] A. A. Saki, M. Alam and S. Ghosh, “Impact of Noise on the Resilience and the Security of Quantum Computing,” *2021 22nd International Symposium on Quality Electronic Design (ISQED)*, Apr. 2021.

[24] S. Rosenblum, P. Reinhold, M. Mirrahimi, L. Jiang, L. Frunzio and R. J. Schoelkopf, “Fault-tolerant detection of a quantum error,” *Science*, vol. 361, no. 6399, pp. 266–270, Jul. 2018.

[25] A. Morea, M. N. Notarnicola and S. Olivares, “Entanglement recovery in noisy binary quantum information protocols via three-qubit quantum error correction codes,” *International Journal of Quantum Information*, vol. 21, no. 07, Feb. 2023.

[26] K. Khan and S. Jain, “Error correction using quantum computation,” *Journal of Digital Science*, vol. 5, no. 1, pp. 12–22, Jun. 2023.

[27] D. Ahadianyah, K. Anwar and G. Budiman, “Investigation on Shor codes as degenerate codes but correct all single quantum errors,” *2022 IEEE Symposium on Future Telecommunication Technologies (SOFTT)*, Nov. 2022.

[28] S. Ling, J. Luo and C. Xing, “Generalization of Steane’s enlargement construction of quantum codes and applications,” *IEEE Transactions on Information Theory*, vol. 56, no. 8, pp. 4080–4084, Aug. 2010.

[29] E. Sabo, A. B. Aloshtous and K. R. Brown, “Trellis decoding for qudit stabilizer codes and its application to qubit topological codes,” *IEEE Transactions on Quantum Engineering*, pp. 1–39, Jan. 2024.

[30] S. Bravyi, M. Englbrecht, R. König and N. Peard, “Correcting coherent errors with surface codes,” *Npj Quantum Information*, vol. 4, no. 1, Oct. 2018.

[31] T. Hu, J. Wu and Q. Li, “SurfaceNet: Fault-Tolerant Quantum Networks With Surface Codes,” in *IEEE Network*, vol. 38, no. 1, pp. 155–162, Jan. 2024.

[32] M. Urbanek, B. Nachman, V. R. Pascuzzi, A. He, C. W. Bauer, and W. A. De Jong, “Mitigating depolarizing noise on quantum computers with noise-estimation circuits,” *Physical Review Letters*, vol. 127, no. 27, Dec. 2021.



**Shani Marish V. Pineda** holds a degree in Bachelor of Science in Computer Engineering from the Polytechnic University of the Philippines. Her academic background has given her a solid foundation in software and systems development, helping her develop the skills to contribute to practical and effective solutions for current and future technological challenges. Passionate about innovation, she aims to advance technology by delivering solutions that improve lives, foster inclusivity, and drive progress, all while embracing continuous learning to create lasting impact.



**Kenneth D. Cabobos** is a Bachelor of Science in Computer Engineering graduate with a specialization in System Development. He is currently working in the field of web development and is passionate about creating innovative solutions and optimizing user experiences. With a strong interest in software development and cloud computing, he continually explores new technologies to enhance his skills and deliver innovative projects.



**Brent Neilson P. Rebulan** is a graduate of Bachelor of Science in Computer Engineering from the Polytechnic University of the Philippines, with a major in Systems Development. He currently leverages his technical expertise in the BPO and RPO industry, excelling at connecting the right people with exceptional work opportunities. Brent's career is distinguished by his ability to optimize recruitment processes through innovative solutions and a deep understanding of complex systems. Known for his collaborative spirit and dedication to excellence, Brent continuously seeks new challenges and opportunities for growth.



**Joshua Benjamin B. Rodriguez**, cum laude, graduated with a Bachelor of Science in Computer Engineering from the Polytechnic University of the Philippines (PUP). He has completed academic units toward a Master of Science in Engineering, specializing in Computer Engineering, at PUP Graduate School. Engr. Rodriguez has been teaching mathematics and computer engineering courses in the College of Engineering for over nine years and is a faculty member of the Department of Computer Engineering within the College of Engineering and Architecture. He serves as the Laboratory Head of Computer Engineering and is recognized for his dedication and innovative teaching methodologies, earning high regard from his students. Engr. Rodriguez is also the adviser of the College of Engineering Honors Society (CEHS) at PUP, a role he has held since 2020, and has been appointed as the adviser of the Association of Computer Engineering Students for Sustainability (ACCESS) for 2024.



**Orland D. Tubola** is currently the Director of the Research Institute for Strategic Foresight and Innovation. He is a licensed Electronics Engineer with a master's degree in Electronics and Communications Engineering from De LaSalle University and is currently taking up his Doctor of Philosophy in Energy Engineering from the University of the Philippines – Diliman. He is also part of two non-government and non-profit organizations. He is the Founding Board of Trustee of Reboot Philippines, a youth organization that advocates for the just transition towards 100% utilization of renewable energy; and he is also the Academic and Content Advisor of Ulap.org, an NGO based in Denmark, that advocates for upskilling of underprivileged youth in the field of cloud computing.